J|A|C|S
COMMUNICATIONS

Published on Web 11/27/2003

Monopod, Bipod, Tripod, and Tetrapod Gold Nanocrystals

Sihai Chen,*,† Zhong Lin Wang,‡ John Ballato,† Stephen H. Foulger,† and David L. Carroll§

Center for Optical Materials Sciences and Engineering Technologies (COMSET), School of Materials Science and Engineering, Clemson University, Clemson, South Carolina 29634-0971, School of Materials Science and Engineering, Georgia Institute of Technology, Atlanta, Georgia 30332-0245, and Center for Nanotechnology, Department of Physics, Wake Forest University, Winston-Salem, North Carolina 27109-7507

Received October 7, 2003; E-mail: chens@clemson.edu

Metal and semiconductor nanoparticles have been extensively studied as active components in a wide variety of basic research and technological applications due to their new or improved optical, electric, and magnetic properties compared to their bulk counterparts.[1] On the basis of their high electric conductivity, metal nanocrystals with higher order complexities such as branched structures, including monopods, bipods, tripods, and tetrapods, are highly desired considering their applications as interconnections in the "bottom-up" self-assembly approach toward future nanocircuits and nanodevices. At present, these kinds of structures are only observed in a series of semiconductor materials such as CdS,[2] CdSe,[3] CdTe,[4] MnS,[5] and ZnO,[6] which are generated through controlled nucleation of a zinc blende-phased core followed by the growth of wurtzite-phased arms having the inherently anisotropic nature of their hexagonal cell structures along the *c*-axis. In these cases, the existence of two kinds of crystal structures within the same nanocrystal (so-called "polytypism") is required. One exception is the case of PbS.[7] Despite being a rock salt-phased semiconductor, metastable multiarmed structures have been observed as transient species toward stable cubes. In all the above cases, harsh conditions such as reactions in organic solvents at high temperatures or chemical vapor deposition are normally required. In this communication, we present the first example of the branched metallic gold nanocrystals synthesized in aqueous solution at room temperature. Since gold has a highly symmetric face-centered cubic (fcc) structure, the formation of single-crystal multiarmed nanostructures in isotropic aqueous solution is quite unexpected. We give high-resolution transmission electron microscopic images, elucidate two types of structural configurations, and discuss their formation mechanisms.

In a typical synthesis, to a 36 mL of cetyltrimethylammonium bromide (CTAB, 0.1 M) solution was added 1.2 mL of 10 mM $HAuCl_4$, 4 μL of concentrated silver plates,[8] and 2.5 mL of 10 mM L-ascorbic acid, the orange color of the Au−CTAB mixture changed to almost colorless after the addition of ascorbic acid (see Figure S1 for the absorption spectra), indicating probably the reduction of Au^{3+} to Au^{+} and/or the formation of complexes. Finally, 0.2 mL of 1 M NaOH was rapidly added to induce the gold nanoparticle formation. Without shaking, the color of the solution changed from slightly blue and finally to purple-red within 1 day.

Figure 1 displayed the TEM image of the obtained particles. Variously shaped particles, including spheres (∼40%), tadpole-like monopods (∼25%), 90° L-shaped, 180° I-shaped, and 120° V-shaped bipods (∼23%), T-shaped, Y-shaped, and regular triangular tripods (∼9%), and cross-like tetrapods (∼3%), are observed. A selected area electron diffraction pattern shown in the inset of

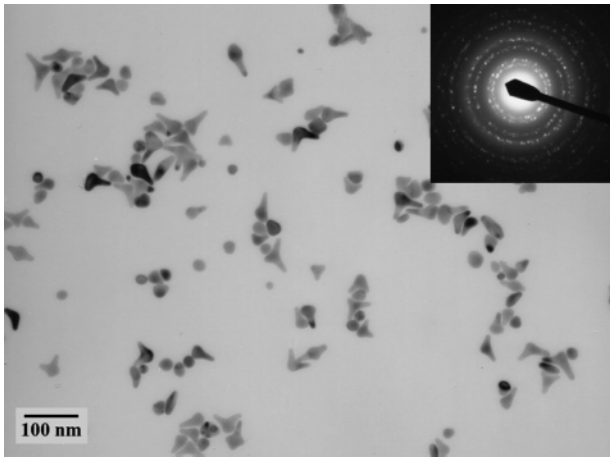

Figure 1. TEM image of the branched gold nanocrystals. The inset shows the corresponding electron diffraction pattern.

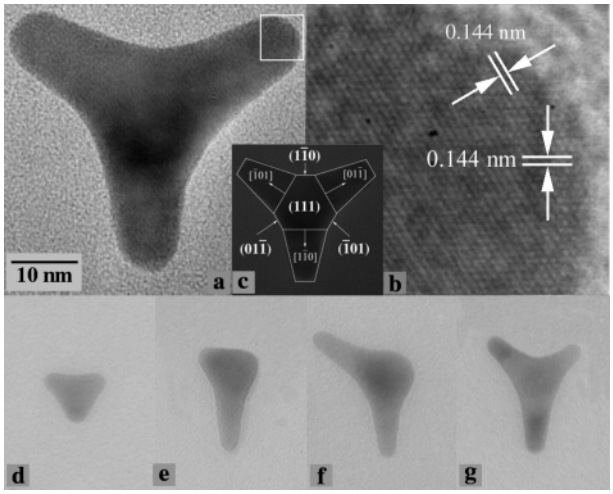

Figure 2. (a) TEM image of a regular tripod nanocrystal and (b) high-resolution image of the pod end as marked by a white frame in panel a. (c) Diagram showing the crystal planes and pod directions. The lower row of panels exhibits the particles developed at various stages: (d) embryo of triangular shape, (e) monopod, (f) V-shaped bipod, and (g) Y-shaped tripod.

Figure 1 clearly demonstrates that these particles have fcc structures. No silver is detected as shown by the elemental analysis (see Figure S2), indicating that these particles are purely gold. Two types of final multipod structures, i.e., regular tripod (Figures 2a) and tetrapod (Figure 3a), can be distinguished. Other particles can be recognized as that formed at different developing stages of pod growth toward these two structures, as displayed in Figure 2d−g and Figure 3d−g, respectively. Since all these particles are collected at the end of the reaction, it is not necessarily said that each particle

† Clemson University.
‡ Georgia Institute of Technology.
§ Wake Forest University.

10.1021/ja038927x CCC: $25.00

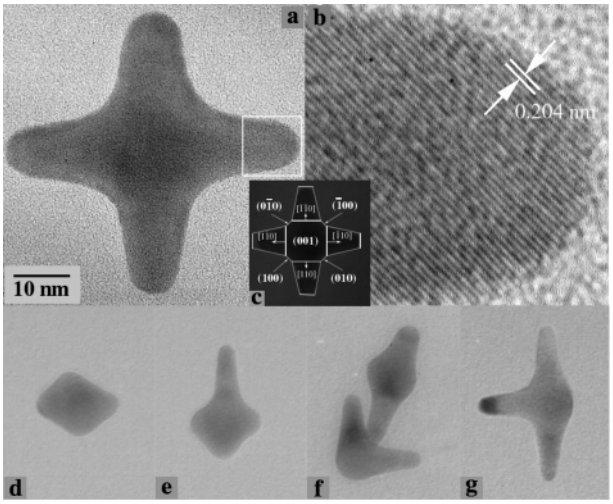

Figure 3. (a) TEM image of a well-developed tetrapod nanocrystal, and (b) high-resolution image of the end of one pod as marked by a white frame shown in panel a. (c) represents a schematic illustration of crystal planes and pod directions. The lower row of panels exhibits the particles developed at various stages: (d) embryo of diamond-like shape, (e) monopod, (f) L-type and I-type bipods, and (g) T-type tripod.

should follow the stepwise pod extrusion process. However, This gradual growth trend should be applicable for most of the particles, as collectively reflected in the absorption spectra (see Figure S3): we found that a 670 nm shoulder peak obtained at 10 min of reaction disappeared after 20 days of aging, corresponding to the increase in symmetry of the nanocrystals from rod-like structures to those having three- or fourfold symmetry axes.

The tripod and tetrapod morphologies are related to their atomic structures. High-resolution TEM studies show that, in both cases, lattice planes continuously extend to the whole particles without stacking faults or twins, indicating they are single crystals. For the tripod particles, perpendicular to each of the three pod growth directions, a lattice plane with interplanar distance of 0.144 nm was measured (Figure 2b), showing that the pod growth occurs preferentially on the {220} planes. It is easy to conclude that the tripod actually lies flat on its (111) plane, with three pods extending in $[1\bar{1}0]$, $[\bar{1}01]$, and $[01\bar{1}]$ directions (Figure 2c). At this point, an interesting question arises: why are only every other three directions out of the six equivalent ⟨110⟩ directions on a {111} basal plane preferentially grown? Considering the structure of gold or silver nanoplates,[8] this may be due to the simultaneous growth inhibition of the {111} and {110} side planes (see Figure S4 for more details).

The high-resolution image shown in Figure 3b gives an interplanar distance of 0.204 nm, which belongs to {200} planes of gold. Considering the geometry of the tetrapod, it is clear that it is oriented along [001] with four pods extruding along $[1\bar{1}0]$, $[\bar{1}\bar{1}0]$, $[\bar{1}10]$, and [110] directions (Figure 3c).

Interestingly, both of the above structures are formed with pod growth along ⟨110⟩ directions, indicating no adsorption or very weak adsorption of molecules (CTAB and/or ascorbic acid) on {110} planes. If strong adsorption occurred on the six {100} plane of the cubic gold, tetrapod structures were formed. On the other hand, if {110} and {111} planes were favorably stabilized at the same time, tripods appeared. The concurrent existence of these two structures may imply the similar interfacial energy of these two planes stabilized by adsorbed molecules.

At this stage, it is not yet clear which components play the main roles in the above actions; however, several points should be addressed. (i) The forced reduction of gold by ascorbic acid through the addition of NaOH is the key step for particle branching. As reported in the previous studies,[9] when gold seeds containing a strong reducing agent of $NaBH_4$ were added at the final step, only spheres or rods were obtained. (ii) The silver nanoplates in our recipe are not necessarily required for branched particle formation; however, the yield is much lower if they are omitted (∼20%). Similar branched particles were also observed in the cases of using other kinds of seeds such as gold (4 nm, aged for one month, yield ∼30%) and silver (15 nm, aged for one month, yield ∼45%). Existence of colloidal silver apparently increases the yields of branched particles; however, direct addition of Ag^+ ions shows a detrimental effect on branded particle formation. This is different from that of the rod growth cases.[10] (iii) A high concentration of CTAB is needed for obtaining the branched particles (see Figure S5 for optical characterization). The self-assembled structures of concentrated CTAB such as rodlike micelles[11] may also play an important role in this case.

In summary, a series of multipod gold nanostructures have been successfully synthesized via a simple chemical reduction method at room temperature. Two types of structurally different particles, i.e., the tripod and the tetrapod, are characterized. These branched particles are expected to have wide applications in nanoelectronics and other related fields.

Acknowledgment. We are thankful for support from DARPA through Grant N66001-03-1-8900 (the Laboratory for Advanced Photonic Composites) and help from Dr. X. Y. Kong for film treatment.

Supporting Information Available: Figures showing the absorption spectra and results of elemental analysis. This material is available free of charge via the Internet at http://pubs.acs.org.

References

(1) *Nanoscale Materials in Chemistry*; Klabunde, K. J., Ed.; John Wiley & Sons: 2001.
(2) (a) Jun, Y. W.; Lee, S. M.; Kang, N. J.; Cheon, J. *J. Am. Chem. Soc.* **2001**, *123*, 5150−5151. (b) Chen, M.; Xie, Y.; Lu, J.; Xiong, Y.; Zhang, S.; Qiang, Y.; Liu, X. *J. Mater. Chem.* **2002**, *12*, 748−753. (c) Joo, J.; Na, H. B.; Yu, T.; Yu, J. H.; Kim, Y. W.; Wu, F.; Zhang, J. Z.; Hyeon, T. *J. Am. Chem. Soc.* **2003**, *125*, 11100−11105.
(3) (a) Manna, L.; Scher, E. C.; Alivisatos, A. P. *J. Am. Chem. Soc.* **2000**, *122*, 12700−12706. (b) Peng, X. *Adv. Mater.* **2003**, *15*, 459−463.
(4) (a) Manna, L.; Milliron, D. J.; Meisel, A.; Scher, E. C.; Alivisatos, A. P. *Nature Mater.* **2003**, *2*, 382−385. (b) Peng, Z. A.; Peng, X. *J. Am. Chem. Soc.* **2001**, *123*, 183−184.
(5) Jun, Y. W.; Jung, Y. Y.; Cheon, J. *J. Am. Chem. Soc.* **2002**, *124*, 615−619.
(6) (a) Iwanaga, H.; Fujii, M.; Ichihara, M.; Takeuchi, S. *J. Crystal Growth* **1994**, *141*, 234−238. (b) Tang, C. C.; Fan, S. S.; de la Chapelle, M. L.; Li, P. *Chem. Phys. Lett.* **2001**, *333*, 12−15. (c) Dai, Y.; Zhang, Y.; Li, Q. K.; Nan, C. W. *Chem. Phys. Lett.* **2002**, *358*, 83−86. (d) Roy, V. A. L.; Djurisic, A. B.; Chan, W. K.; Gao, J.; Lui, H. F.; Surya, C. *Appl. Phys. Lett.* **2003**, *83*, 141−143.
(7) Lee, S. M.; Jun, Y. W.; Cho, S. N.; Cheon, J. *J. Am. Chem. Soc.* **2002**, *124*, 11244−11245.
(8) Silver plates, with an average size of 220 nm and a thickness of 25 nm, were synthesized according to a modified previous method; see: (a) Chen, S.; Carroll, D. L. *Nano Lett.* **2002**, *2*, 1003−1007. (b) Chen, S.; Fan, Z.; Carroll, D. L. *J. Phys. Chem. B* **2002**, *106*, 10777−10781.
(9) (a) Jana, N. R.; Gearheart, L.; Murphy, C. J. *Langmuir* **2001**, *17*, 6782−6786. (b) Jana, N. R.; Gearheart, L.; Murphy, C. J. *J. Phys. Chem. B* **2001**, *105*, 4065−4067. (c) Jana, N. R.; Gearheart, L.; Murphy, C. J. *Adv. Mater.* **2001**, *13*, 1389−1393.
(10) Kim, F.; Song, J. H.; Yang, P. *J. Am. Chem. Soc*. **2002**, *124*, 14316−14317.
(11) Tornblom, M.; Henriksson, U. *J. Phys. Chem. B* **1997**, *101*, 6028−6035.

JA038927X